Semiactive Seismic Isolation System Using Controllable Friction Damper

by

Takafumi FUJITA[1], Mamoru SHIMAZAKI[1], Yutaka HAYAMIZU[2],
Satoru AIZAWA[2], Masahiko HIGASHINO[2] and Nobuyoshi HANIUDA[3]

1. INTRODUCTION

Current passive seismic isolation techniques are now capable of nearly satisfying demands in respect of reduction of response acceleration, but regarding relative displacement, its reduction is desired. For this reason, the authors have developed controllable friction dampers, proposed a seismic isolation structure which has introduced semiactive control by using them, and have carried out studies for decreasing relative displacement without decreasing the seismic isolation effect. This paper summarizes test results of the semiactive seismic isolation structure using controllable friction dampers [1, 2], and the examination result for braking control which uses controllable friction dampers as braking equipment [3]. The purpose of this study is to develop an intelligent seismic isolation structure which will demonstrate the optimal seismic isolation effect within the allowable relative displacement of a base-isolated structure.

2. BASIC EXAMINATION OF SEMIACTIVE SEISMIC ISOLATION STRUCTURE USING DAMPING FORCE-CONTROLLABLE DAMPER

2.1 Semiactive Control Rule Based on Optimal Regulator

An analytical model of two mass system is considered [Fig. 1]. Equations of motion can be described as follows:

$$m_1\ddot{x}_1+c_1\dot{x}_1+c_2(\dot{x}_1-\dot{x}_2)+k_1x_1+k_2(x_1-x_2)+F = -m_1\ddot{z} \quad (1)$$

$$m_2\ddot{x}_2+c_2(\dot{x}_2-\dot{x}_1)+k_2(x_2-x_1) = -m_2\ddot{z} \quad (2)$$

where

- x_1: relative displacement of building floor slab to ground surface
- x_2: relative displacement of building roof slab to ground surface
- m_1: mass of building floor slab
- m_2: mass of building roof slab
- $\ddot{z}$: seismic motion acceleration
- k_1: spring constant of rubber bearing
- c_1: damping constant of rubber bearing
- k_2: spring constant of building
- c_2: damping constant of building
- F : damping force by damping force-controllable damper

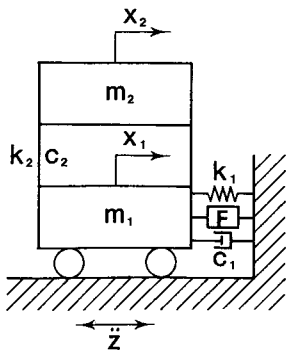

Fig. 1 Analytical model

Aiming at reduction in absolute acceleration and relative displacement, performance index J is set as follows (provided, however, that $u = F$):

[1] Institute of Industrial Science, University of Tokyo

[2] Takenaka Corporation

[3] Kayaba Industry Co., Ltd.

$$J = \int_0^\infty \{\alpha_1(\ddot{x}_1+\ddot{z})^2+\alpha_2(\ddot{x}_2+\ddot{z})^2+\beta x_1^2+\gamma u^2\}dt \tag{3}$$

The optimal regulator problem, consisting of Eqs. (1), (2) and (3), is solved and the optimum control force u^* is obtained.

When semiactive control by the damping force-controllable damper is considered, the direction of force that can be generated by the damper is dependent upon the direction of relative velocity; hence the actual control force follows the conditions shown below:

$$u = \begin{cases} u^* & (u^* \cdot \dot{x}_1 > 0) \\ 0 & (u^* \cdot \dot{x}_1 \leq 0) \end{cases} \tag{4}$$

2.2 Comparison between Active Control and Semiactive Control

In order to examine the performance of semiactive seismic isolation based on the above-mentioned control rule, a comparison between passive seismic isolation and ordinary active seismic isolation—which has not received restrictions shown in Eq. (4)—was made by simulation.

The results, when the weights of the performance index are changed and reduction in absolute acceleration was aimed at and when reduction in relative displacement was aimed at, are shown in Figs. 2 and 3, respectively. These two figures indicate the following: As shown in Fig. 2, semiactive control cannot drastically decrease response acceleration (rather response displacement increases), but as shown in Fig. 3, the seismic isolation effect was the same as that of passive control, and further decreased the response displacement. This means that force which can realized such control can be generated by the damping force-controllable damper, and viewed from the cost and reliability, the semiactive control is more advantageous than the active control.

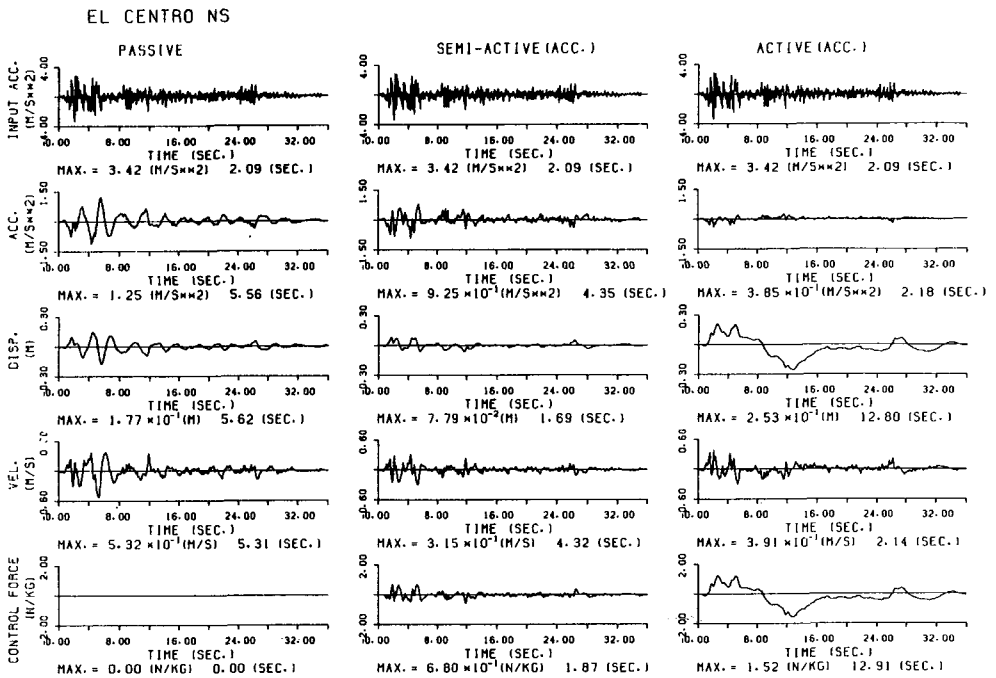

Fig. 2 Simulation results for passive, semiactive and active isolation systems when reduction in response acceleration aimed at.

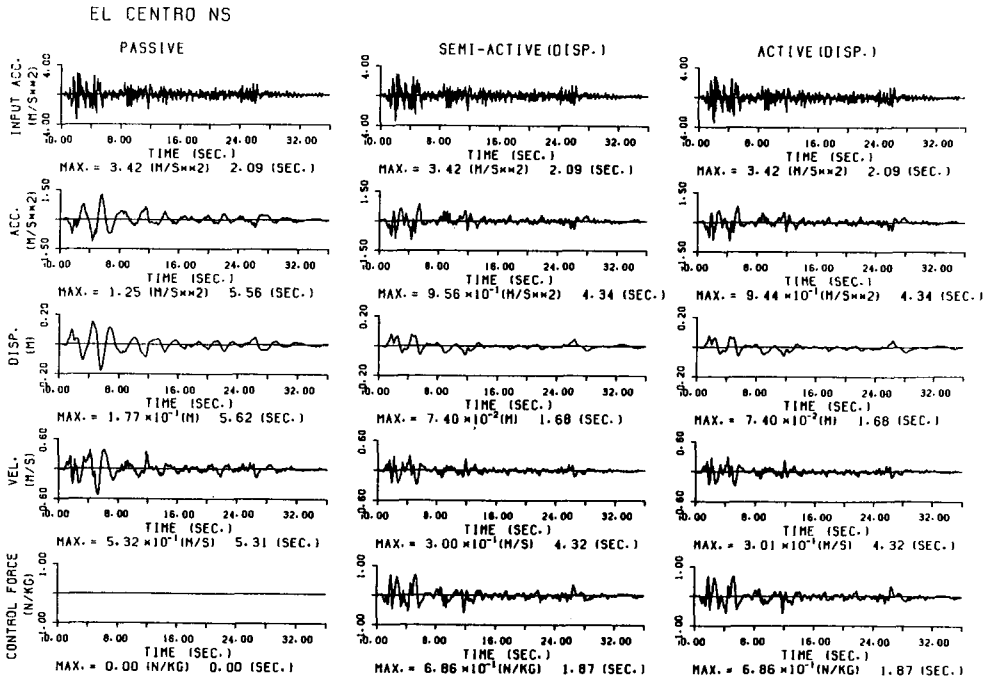

Fig. 3 Simulation results for passive, semiactive and active isolation systems when reduction in response displacement aimed at.

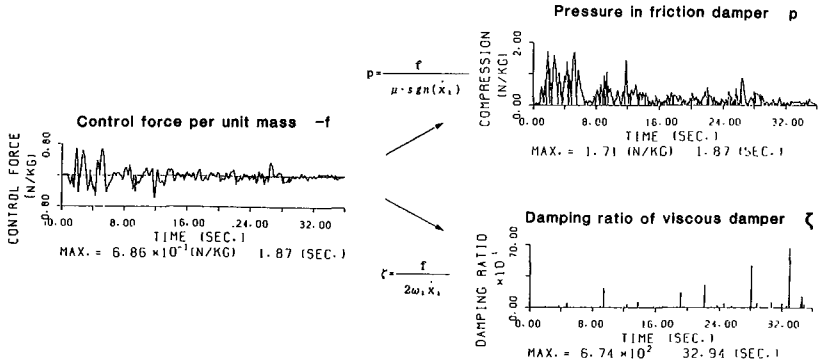

Fig. 4 Comparison between friction damper and viscous damper

2.3 Examination about Damping Force-controllable Damper

Figure 4 is a comparison between the case of realizing semiactive control force (per unit mass) of Fig. 3 by the friction damper and the case of realizing the semiactive control force by a viscous damper. According to this comparison, pressing force in the case of the friction

damper can be realized by an ordinary hydraulic actuator, etc., but the maximum value of the damping ratio in the case of the viscous damper becomes a stupendous value far exceeding the critical damping ratio, and it is considered difficult to be realized by conventional hardware. In the present study, therefore, it was decided to adopt the controllable friction damper using a hydraulic actuator as the controllable damper for semiactive seismic isolation.

3. SEMIACTIVE SEISMIC ISOLATION STRUCTURE USING CONTROLLABLE FRICTION DAMPER

3.1 Analytical Model

If the controllable damper is decided to be a controllable friction damper in the analytical model of Fig. 1, equations of motion will be as shown below, considering changeover of static/dynamic friction due to the presence or absence of sliding of the friction damper.

(1) When there is no sliding of friction damper — Phase I

$$x_1=\text{const.},\quad \dot{x}_1=0 \tag{5}$$

$$\ddot{x}_2+2\zeta_2\omega_2(\dot{x}_2-\dot{x}_1)+\omega_2^2(x_2-x_1)=-\ddot{z} \tag{6}$$

(2) When there is sliding of friction damper — Phase II

$$\ddot{x}_1+\frac{1}{1-\rho}\left\{2\zeta_1\omega_1\dot{x}_1+2\rho\zeta_2\omega_2(\dot{x}_2-\dot{x}_1)+\omega_1^2x_1+\rho\omega_2^2(x_1-x_2)+\mu p\cdot\mathrm{sgn}(\dot{x}_1)\right\}=-\ddot{z} \tag{7}$$

$$\ddot{x}_2+2\zeta_2\omega_2(\dot{x}_2-\dot{x}_1)+\omega_2^2(x_2-x_1)=-\ddot{z} \tag{8}$$

(3) Changeover condition from Phase I to Phase II

$$\left|\ddot{z}+\frac{1}{1-\rho}\left\{2\rho\zeta_2\omega_2\dot{x}_2+\omega_1^2x_1+\rho\omega_2^2(x_1-x_2)\right\}\right|>\frac{\mu p}{1-\rho} \tag{9}$$

(4) Changeover conditions from Phase II to Phase I

$$\dot{x}_1=0 \text{ and}$$

$$\left|\ddot{x}_1+\ddot{z}+\frac{1}{1-\rho}\left\{2\rho\zeta_2\omega_2\dot{x}_2+\omega_1^2x_1+\rho\omega_2^2(x_1-x_2)\right\}\right|\leq\frac{\mu p}{1-\rho} \tag{10}$$

where

$$\omega_1=\sqrt{\frac{k_1}{m_1+m_2}},\ \zeta_1=\frac{c_1}{2\sqrt{(m_1+m_2)k_1}},\ \omega_2=\sqrt{\frac{k_2}{m_2}},\ \zeta_2=\frac{c_2}{2\sqrt{m_2k_2}},$$

$$\rho=\frac{m_2}{m_1+m_2},\ \mu p=\frac{F}{m_1+m_2}$$

Further dynamic characteristics of the controllable friction damper (hydraulic actuator) shall be expressed by

$$T\dot{p}+p=Ku \tag{11}$$

where T is a time constant and K is a gain.

Therefore, from Eqs. (7), (8), and (11), the system becomes a 5th order one, and the semiactive control rule applies to this system.

3.2 Semiactive Control Rule

It is very difficult to actually observe all five state variables for the sake of control. In general practice, the state variables are estimated by an observer, but when the observer is used, it is known that control results will deteriorate and the robustness will decrease. As a control rule for practical use, therefore, the order of the model is reduced as follows:

$$\ddot{x}+2\zeta\omega\dot{x}+\omega^2x+\mu p=-\ddot{z} \tag{12}$$

$$T\dot{p}+p=Ku \tag{13}$$

$$J=\int_0^\infty\left\{a(\ddot{x}+\ddot{z})^2+\beta x^2+ru^2\right\}dt \tag{14}$$

where

$$x = x_1 = x_2,\ \omega = \sqrt{\frac{k_1}{m_1+m_2}},\ \zeta_1 = \frac{c_1}{2\sqrt{(m_1+m_2)k_1}},\ \zeta_1 = \frac{c_1}{2\sqrt{(m_1+m_2)k_1}},\ \mu p = \frac{F}{m_1+m_2}$$

In this case, the system becomes a 3rd order system, and relative displacement and pressing force from the three state variables are directly measured by a displacement transducer and a pressure transducer, and relative velocity is obtained by a simple differential operation as follows:

$$\hat{\dot{x}}(t) = \frac{x(t)-x(t-\Delta t)}{\Delta t} \tag{15}$$

This method is justified by the following reasons: In a seismic isolation system, hardly no difference is observed in response displacement and response velocity between the upper and lower parts of a building; hence it is alright to assume that the building is a rigid body. In the seismic isolation system, the motion of relative displacement is of a considerable long period; hence relative velocity can be estimated with considerable precision by simple differential operation as shown in Eq. (15). Since this method may be interpreted, in a sense, as an approximate complete-state feedback control, excellent robustness can be expected which is a characteristic of the complete state feedback.

Further it has been confirmed that this control method has, by simulation, almost nearly the same performances as those of the complete state feedback in which all five state quantities are observed.

4. DEVELOPMENT OF CONTROLLABLE FRICTION DAMPER

The controllable friction damper (Fig. 5) developed in the present study obtains controllable damping by controlling the pressing force of the friction material (copper-based ceramics). Its two ends are fixed to the bottom surface of the building floor slab and to the ground surface, respectively. The maximum friction force is 39.2 kN, which is a sufficient capacity for the purpose of the present study, and it is greatly advantageous that contrary to the viscous damper, damping force can be applied to the system regardless of the magnitude of velocity (for the semiactive control, this is an important matter). The friction coefficient is 0.53, and through the use of a spherical bearing, a force other than in the exciting direction (horizontal single axis) is lost. Further, as a result of performance tests, it has been confirmed that the damping force is proportionate to the pressing force, and is independent of the sliding velocity and the sliding direction.

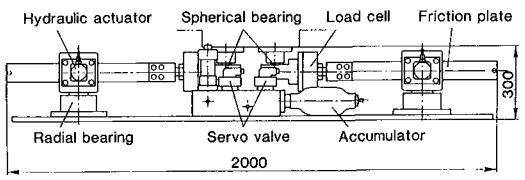

Fig. 5 Controllable friction damper

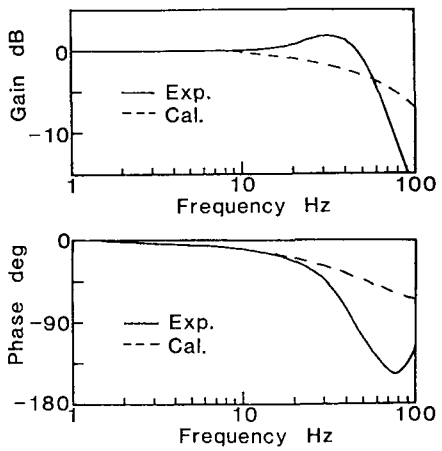

Fig. 6 Dynamic characteristics of controllable friction damper

Fig. 6 shows the dynamic characteristics of the controllable friction damper. The solid line is the experimental value by dynamic characteristic confirmation tests, and the broken line shows a theoretical value, when the dynamic characteristic is made into a model of a first order system, assuming that time constant T = 0.004 s (4 ms). As long as the test result shows, the dynamic characteristic of the controllable friction damper is considered to be of a higher order

vibration characteristic. In 10 Hz or below, however, both the gain and phase characteristics are excellently approximated, which is a frequency range sufficient for the controllable friction damper.

5. VIBRATION CONTROL TEST

5.1 Building Model

The building model (Fig. 7) used in the test consists of a steel skeleton frame and a steel plate weight, and is supported by four multistage rubber bearings. Its total weight is 5,250 kg, its first mode natural frequency and damping ration are 0.54 Hz and 1.9%, respectively, in the both x-direction and y-direction, while those for the second mode are 4.1 Hz and 0.9%, respectively, in the x-direction and 19.5 Hz and 0.8%, respectively, in the y-direction. The allowable relative displacement is 0.1 m.

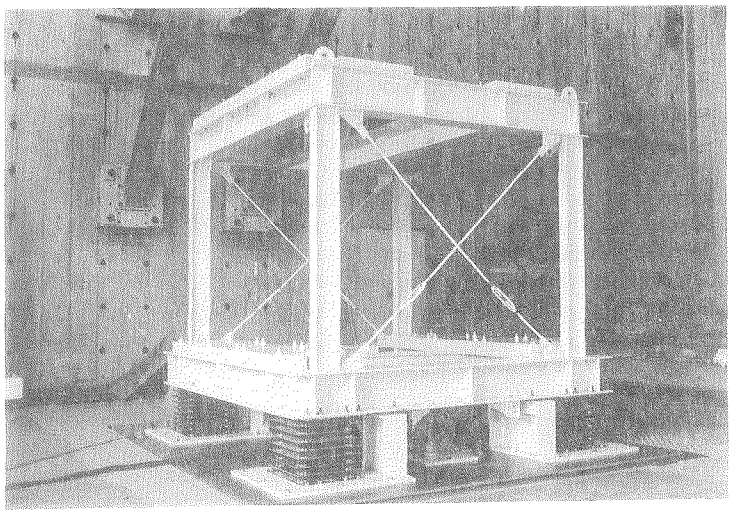

Fig. 7 Experimental model

5.2 Control System

The control system (Fig. 8) consists of a 32-bit personal computer, a sensor, A/D and D/A converters, etc. The sampling period is 10 ms, and is accurately controlled by a interrupt timer. The control voltage calculated by the computer is inputted into the servo amplifier to actuate the controllable friction damper. The control program is described in Turbo C.

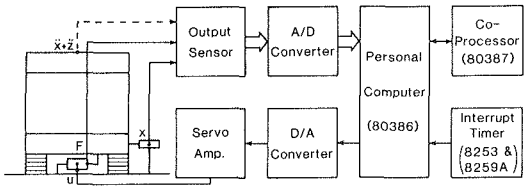

Fig. 8 Control system

5.3 Test Results

Figure 9 shows the relations of input seismic acceleration, absolute acceleration, and respective maximum response values in the El Centro NS input. Passive 1 and Passive 2 in the figure indicate passive seismic isolation by the friction dampers of constant pressing forces, and the pressing force of Passive 2 is stronger. Semiactive in the figure indicates standard semiactive control. According to this, the responses of the semiactive system are nearly linear, but these of the passive systems are nonlinear. Further, in the semiactive system, conflicting relative displacement and absolute acceleration are satisfactorily suppressed, but in the passive systems, it is indicated that they cannot be decreased simultaneously.

Figure 10 shows the time-histories in the case of inputting El Centro NS 300 Gal. The performance of the passive system in such a case is the standard one of the conventional system, but the semiactive system has the same seismic isolation effect as the passive system, and has reduced the relative displacement into half. The test and analysis have excellent agreement,

indicating the validity of the model.

Figure 11 shows the result of a frequency analysis of the result of Fig. 10, and indicates a transfer function of the response acceleration and a Fourier spectrum of the response displacement. These indicate that the excellent performance of semiactive seismic isolation is being shown from the frequency area. Further, in the semiactive system, the clear peak, as in the passive system, is not shown in the transfer function; hence it is possible to expect a sufficient seismic isolation effect against earthquakes having any frequency components.

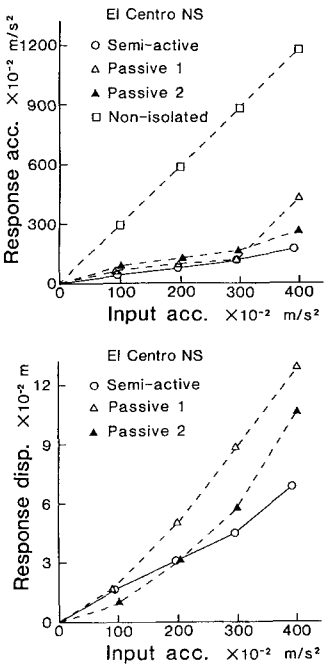

Fig. 9 Response acceleration and displacement of semiactive system (comparison with those of passive and non-controlled systems)

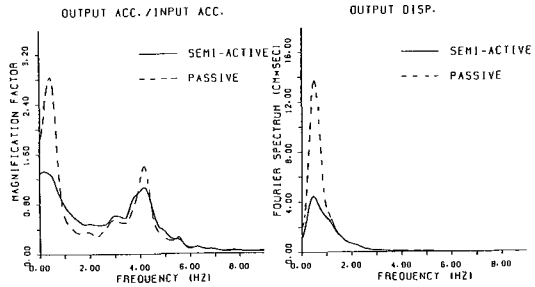

Fig. 11 Performance of semiactive system in frequency domain

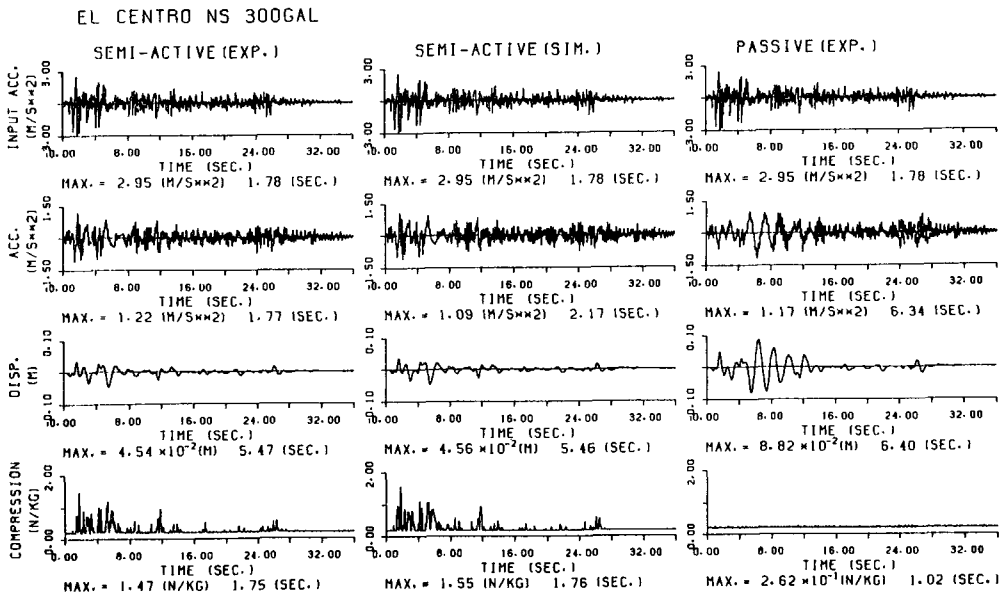

Fig. 10 Time histories of responses of semiactive and passive system (experimental and analytical results)

6. BRAKING CONTROL USING CONTROLLABLE FRICTION DAMPERS

It has been verified that the semiactive seismic isolation structure, using controllable friction dampers, has the same seismic isolation effect as that of the conventional passive seismic isolation structure, and can suppress response displacement. In the semiactive control by a single feedback gain, however, response displacement also increases as input seismic motion becomes greater. Consequently, if an excessively great seismic motion occurs, in which response displacement exceeds a critical displacement, not only the seismic isolation effect will be lost but also serious damage will occur by the collision of the seismic isolation building with the surrounding structures. Consequently, by properly changing over multiple feedback gains and by using the controllable friction dampers as braking equipment against excessively great seismic motion inputs, it is hoped to implement braking control which suppresses response displacement within an allowable displacement, even if slightly sacrificing the seismic isolation effect, and to evade collision with the surrounding structures. This chapter analyses this, using the test model.

6.1 Feedback Changeover by Fuzzy Rule

To the changeover of feedback gains in braking control, the fuzzy rule is applied. For fuzzy variables, response velocity and response displacement are used. Table 1 shows the control rule. Further, the membership functions of various fuzzy variables are shown in Fig. 12. The adaptability of the respective control rules are defined by the product of membership function values of various fuzzy variables, and their weighted average values are considered to be the entire inference results. On the basis of these results, outputs are fuzzy-divided into the input space as shown in Fig. 13. Further, in the present analysis, braking control is effected by the changeover of two kinds of feedback gains, and even when several kinds of feedback gains are used, this method can be similarly applied.

Rule	X	$\dot{X}$	u
1	NB	----	H
2	NM	NB,NM,PB	H
3	NM	S,PM	N
4	S	NB,PB	H
5	S	NM,S,PM	N
6	PM	NB,PM,PB	H
7	PM	NM,S	N
8	PB	----	H

NB : Negative Big , NM : Negative Medium ,
S : Small , PM : Positive Medium , PB : Positive Big ,
N : Normal Gain , H : High Gain

Table 1 Fuzzy rules

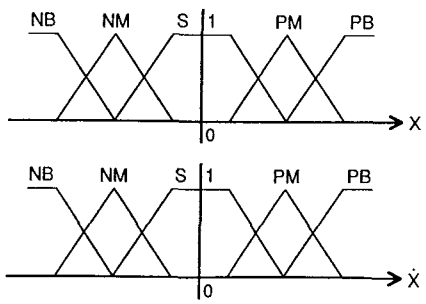

Fig. 12 Membership functions

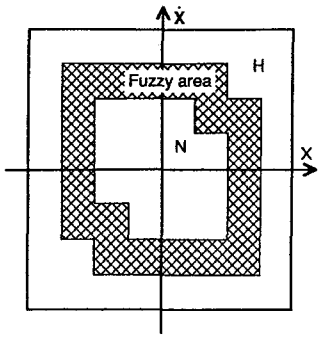

Fig. 13 Fuzzy area in input-plane

6.2 Simuration Results

For the analysis, El Centro NS wave and Akita NS waves have been used as input seismic motions. Analysis results are shown in Figs. 14 and 15. The indicated by the solid lines in the

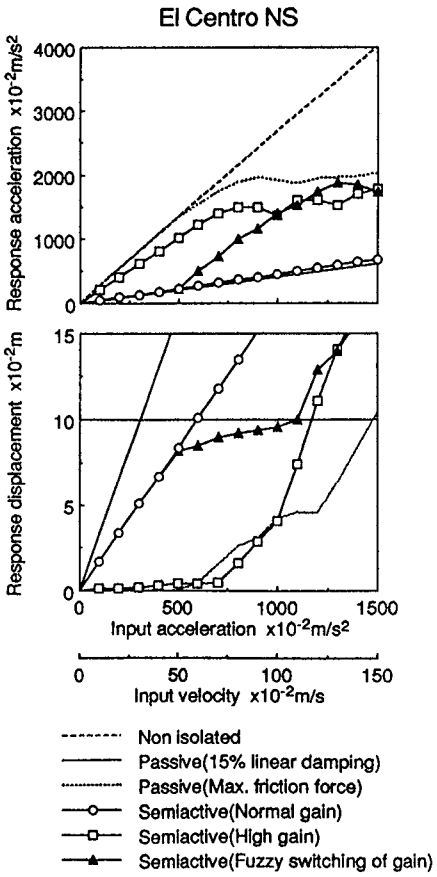

Fig. 14 Simulation results for braking control (El Centro NS input)

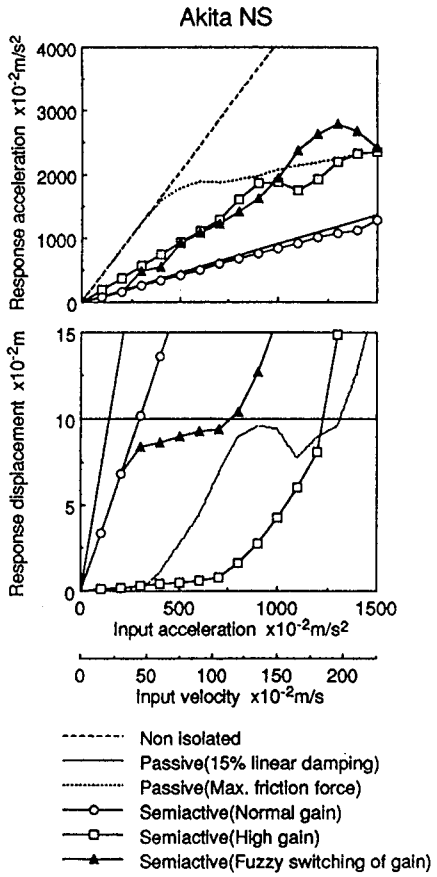

Fig. 15 Simulation results for braking control (Akita NS input)

Figures are the passive responses, when the system has a 15% linear damping, which is optimal damping for the passive seismic isolation, but there are many difficulties to actually giving linear damping of 15% to the building. This ideal passive seismic isolation system demonstrates a sufficient seismic isolation effect, but when the input velocity of seismic motions rise to about 25 kine, the allowable displacement is reached. Further, Passive shown by a broken line in the figures is the maximum friction force, which the controllable friction damper can demonstrated and is also the Passive response, when the friction force is made constant. This Passive response shows the maximum capacity, when the controllable damper is used as braking equipment. For instance, in the case of El Centro NS waves, allowable displacement is reached, when input velocity rises to about 150 kine. Consequently, this indicates that whatever kind of control is made, it is impossible to suppress the response within allowable displacement against input above a displacement of 150 kine.

Allowable displacement in the present analysis is 0.1 m, and braking control has been effected by changeover of two kinds of feedback gains. Namely, emphasis is laid normally on the seismic isolation effect, and a weak gain is used so that the maximum seismic isolation effect can be demonstrated, and as the seismic motion input becomes greater and is liable to exceed allowable displacement, a strong gain is used by placing emphasis on displacement suppression. In the selection of the respective gains, the gain, which is used for ordinary semiactive control (Normal gain in the figures), is used for a weak gain. This gain has the same seismic isolation effect as that of the ideal passive seismic isolation gain, reduces response

displacement into half. The reason for using this gain is that in the semiactive seismic isolation, there is a limit to the acceleration reducing capacity, however weak the gain is made, and this limit is about the same as that by the ideal passive seismic isolation system. For a strong gain, on the other hand, the authors have used at this time a gain (High gain in the figures) that can suppress response displacement within an allowable value against the seismic motion up to an input velocity of about 100 kine, by braking control. Provided, however, that this is a limit to the capacity of the controllable friction damper; hence even if the control system demands a large operation quantity that exceeds such a limit, the capacity of the system's maximum value is saturated. Through braking control using the changeover of these two kinds of gains, allowable displacement is exceeded at about 50 kine of input velocity, against seismic motion waves at both sides by semiactive control using a single gain, but the response displacement is suppressed within the allowable value up to an input velocity of 100 kine. Moreover, until the gain changeover occurs, the same seismic isolation effect as that of the ideal passive seismic isolation system has been demonstrated. The only concern is that when the gain changeover occurs, the seismic isolation effect is sacrificed for the sake of displacement suppression, but in the ideal passive seismic isolation and semiactive control, the seismic isolation effect will decrease, when response displacement reaches allowable displacement, and finally a collision with the surrounding building will occur, and the response acceleration is considered to become larger than the state of non-seismic isolation. Compared with such a situation, it can be said that the semiactive control has a considerable seismic isolation effect.

Figure 16 shows the response wave forms at the time of braking control by the El Centro NS wave input. The control pattern in the figure shows what are used for the gain, and it indicates that when acceleration is 0, the normal gain is used, when acceleration is 1, a high gain is used and when acceleration is 0.5, it is the fuzzy area. From the same figure, it can be realized that when response displacement is about to exceed allowable displacement, by braking the gain, the gain changeover occurs, and response displacement is suppressed within the allowable value little trouble.

In this analysis, seismic motions up to an input velocity of 100 kine is considered, and as a result, two kinds of feedback gains have been selected. It is considered that through this method, the number of feedback gains can be examined, if allowable displacement and the design seismic motion level are given, and the same result can be obtained by the selection of feedback gains.

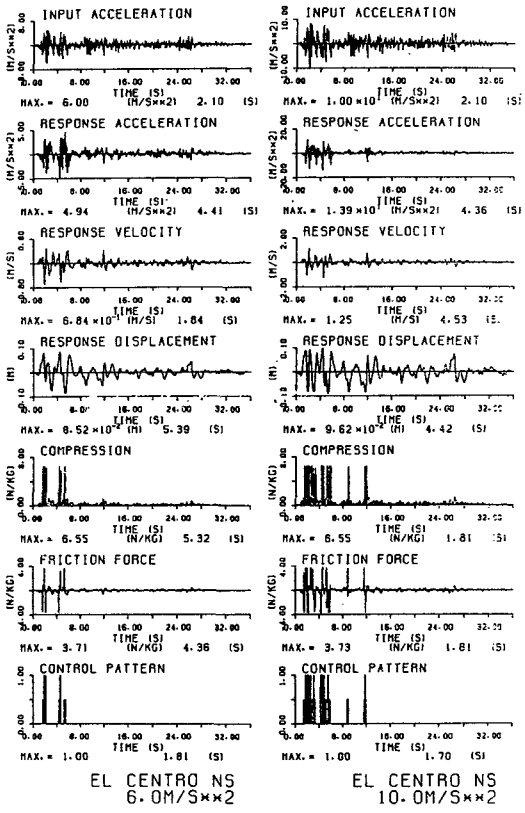

Fig. 16 Responses of semiactive system with braking control

7. CONCLUSION

Aiming at the optimal seismic isolation effect within the allowable relative displacement of the seismic isolation structure, the authors have developed the controllable friction damper, proposed a seismic isolation structure which introduces a semiactive control using the controllable

friction damper and obtained the following results:
(1) It has been verified that the present seismic isolation structure has the same seismic isolation effect as that of the conventional passive seismic isolation system and lowers response displacement.
(2) It has been shown that the damping force-controllable friction damper using a hydraulic actuator is effective in semiactive seismic isolation.
(3) As a control rule for semiactive seismic isolation, it has been shown that the control rule, which uses the features of a seismic isolation structure based on the optimal regulator, is effective.
(4) It has been confirmed by analyses that braking control can suppress response displacement to within allowable displacement, while attaching importance to the seismic isolation effect even in the case of excessively large seismic motion of the level which far exceeds the design standard of the current seismic isolation structure.

REFERENCES

[1] T.Fujita, K. Kabeya, Y.Hayamizu, S.Aizawa, M.Higashino, T.Kubo, No.Haniuda and T.Mori, Semi-Active Seismic Isolation System Using Controllable Friction Damper (1st Report, Development of Controllable Friction Damper and Fundamental Study of Semi-Active Control System), Trans. of JSME, Vol.57, No.536, Ser.C, pp1122-1128, April 1991 (in Japanese).
[2] T.Fujita, M.Shimazaki, Y.Hayamizu, S. Aizawa, M.Higashino, T.Kubo and No.Haniuda, Semiactive Seismic Isolation System using controllable Friction damper (2nd Report, Study of the System with Distributed Controllable Friction Dampers), Trans. of JSME, Vol.58, Ser.C, pp2012-2016, July 1992 (in Japanese).
[3] M.Shimazaki and T.Fujita, Branking Control of Semiactive Seismic Isolation System Using Controllable Friction Damper, SEISAN-KENKYU, Vol.44, No.10, pp509-512, October 1992 (in Japanese).